Eur. Phys. J. B **31**, 489–494 (2003)
DOI: 10.1140/epjb/e2003-00058-x

THE EUROPEAN PHYSICAL JOURNAL B

Density matrix theory of population inversion in biased semiconductor superlattices

P. Kleinert[1,a] and V.V. Bryksin[2]

[1] Paul-Drude-Institut für Festkörperelektronik, Hausvogteiplatz 5–7, 10117 Berlin, Germany
[2] Physical Technical Institute, Politekhnicheskaya 26, 194021 St. Petersburg, Russia

Received 25 October 2002 / Received in final form 27 November 2002
Published online 6 March 2003 –

Abstract. The field-induced carrier redistribution between the subbands of a semiconductor superlattice is treated using the density matrix approach. The unit cell of the superlattice consists of one quantum well with three occupied subbands. Carrier scattering on polar-optical phonons is described within the microscopic bulk phonon model. At the tunneling resonance, an intrinsic population inversion is observed. The temperature dependence of the population inversion is determined.

PACS. 73.40.Gk Tunneling – 73.50.Fq High-field and nonlinear effects

1 Introduction

The study of interminiband effects in superlattices (SLs) is a topic of continued interest since the invention of quantum cascade lasers (QCLs) [1]. These devices consist of a SL, the unit cell of which contains typically up to 20 layers. This has to be contrasted with the original work by Kazarinov and Suris [2], who proposed an implementation of unipolar mid-infrared lasers based on a SL with a unit cell consisting of a single well and barrier. The recent demonstration of a staircase laser [3] goes in the direction of the original proposal to simplify the design concept by reducing the number of quantum wells within the SL unit cell considerably. Almost all other QCLs consist of complex multilayer structures characterized by a periodic alternation of carrier injectors and active regions, in which the infrared radiation is generated. The search for simple mid-infrared laser structures offers the advantage to study basic physical properties of the field-induced carrier repopulation on an analytically tractable model with a simple SL cell.

Unfortunately, most theoretical approaches, which used numerical Monte Carlo simulations [4–7] or approximate rate equations [8–12], focused on the simulation of the existing complex devices, but did not search for simple laser designs based on a multisubband SL. Only recently, such a study has been initiated on the basis of the density-matrix approach [13,14]. In these papers, based on the tight-binding model, a SL with three subbands has been considered. Treating tunneling *via* the off-diagonal elements of the density matrix and scattering-induced carrier transitions within the constant relaxation-time approximation, the field dependence of the carrier redistribution between the subbands has been calculated. It has been found that, at the tunneling resonance, a global intrinsic population inversion may occur, which can be used to fabricate injectorless QCLs based on SLs with a simple unit cell. Unfortunately, our previous approach [13,14] has the disadvantage that scattering was treated in the simple constant relaxation-time approximation. Such an approximation introduces many scattering time parameters and allows the treatment of the temperature dependence only in a phenomenological manner. This disadvantage will be partly removed in the present paper by treating scattering in a more realistic fashion starting from a microscopic model. This allows a study of the temperature dependence of the field-induced carrier redistribution in more detail.

2 Basic theory

The biased multiband SL is described by a tight-binding Hamiltonian, in which the coupling between nearest neighbour wells creates minibands, whose widths are denoted by Δ_ν. We will focus on a SL with three subbands ($\nu = 1, 2, 3$) as can be realized by only a few layers within the SL unit cell. In the limit of low carrier densities (when the Boltzmann statistics approximately applies), the elements $f_\nu^{\nu'}$ of the density matrix are solutions of the kinetic equations

$$\left\{ \frac{e}{\hbar} E \nabla_{k_z} + \frac{\mathrm{i}}{\hbar} \left[\varepsilon_{\nu'}(\boldsymbol{k}) - \varepsilon_\nu(\boldsymbol{k}) \right] \right\} f_\nu^{\nu'}(\boldsymbol{k}) + \frac{\mathrm{i}eE}{\hbar} \sum_\mu \left[Q_{\mu\nu}(\boldsymbol{k}) f_\mu^{\nu'}(\boldsymbol{k}) - Q_{\nu'\mu}(\boldsymbol{k}) f_\nu^\mu(\boldsymbol{k}) \right] = \sum_{\mu\mu'} \sum_{\boldsymbol{k}_1} f_\mu^{\mu'}(\boldsymbol{k}_1) W_{\mu\nu}^{\mu'\nu'}(\boldsymbol{k}_1, \boldsymbol{k}), \quad (1)$$

[a] e-mail: kl@pdi-berlin.de

with E denoting the electric field. In our previous approach [13,14], the intra- and inter-subband scattering probabilities $W_{\mu\nu}^{\mu'\nu'}(\boldsymbol{k}_\prime, \boldsymbol{k})$ have been treated within the phenomenological relaxation-time approximation. It is the aim of the present approach to overcome this limitation. The microscopic description of scattering provides more reliable data concerning the field-induced carrier redistribution and, therefore, enhances the predictive capacity of our approach. The subband energy dispersion relations of the considered model are assumed to have the simple form

$$\varepsilon_1(\boldsymbol{k}) = \frac{\hbar^2 \boldsymbol{k}_\perp^2}{2m^*} + \frac{\Delta_1}{2}\left(1 - \cos k_z d\right), \tag{2}$$

$$\varepsilon_2(\boldsymbol{k}) = \frac{\hbar^2 \boldsymbol{k}_\perp^2}{2m^*} + \varepsilon_{g_1} + \Delta_1 + \frac{\Delta_2}{2}(1 + \cos k_z d), \tag{3}$$

$$\varepsilon_3(\boldsymbol{k}) = \frac{\hbar^2 \boldsymbol{k}_\perp^2}{2m^*} + \varepsilon_{g_1} + \varepsilon_{g_2} + \Delta_1 + \Delta_2 + \frac{\Delta_3}{2}(1 - \cos k_z d), \tag{4}$$

where only one effective mass m^* is used to characterize the lateral carrier motion. ε_{g_1} and ε_{g_2} are the energy gaps between the subbands 1, 2 and 2, 3, respectively. The elements of the dipole matrix

$$Q_{\mu\mu'}(\boldsymbol{k}) = \sum_{\boldsymbol{K}} \chi_{\mu'}(\boldsymbol{k}+\boldsymbol{K}) \nabla_{k_z} \chi_\mu^*(\boldsymbol{k}+\boldsymbol{K}) \tag{5}$$

couple the subbands to each other *via* the off-diagonal elements of the density matrix. $Q_{\mu\mu'}(\boldsymbol{k})$ is calculated from the SL envelope functions $\chi_\mu(\boldsymbol{k}+\boldsymbol{K})$, with $\boldsymbol{K}$ being a vector of the reciprocal lattice. On the right hand side of equation (1), various components of the scattering probability appear, which are associated with intra- and intersubband carrier transitions. We will treat scattering on polar-optical bulk phonons. The simple bulk phonon model has not been chosen for an accurate description of real systems. Rather, it is our intent here to use a sufficiently simple model for analytical considerations to demonstrate qualitative features in the field-induced carrier redistribution. We will focus on an explicit description of scattering probabilities that describe hopping like transitions in the Wannier-Stark picture. In Appendix A, expressions for these terms are presented in a form, which allows a detailed analysis of intracollisional field effects [15] and the associated electro-phonon resonances [16]. As these quantum effects are certainly unimportant for the laser operation, we will neglect the field dependence of the scattering in our numerical work.

The solution of the kinetic equation (1) is searched for in the regime of strong electric fields, when resonant tunneling between adjacent wells can occur. In this regime, we switch to the Wannier-Stark (WS) representation and retain the most dominant intracell contributions of the density matrix. This approximation is justified under the condition that the states are sufficiently localized so that the inequality $\Omega\tau_{eff} > 1$ is satisfied ($\Omega = eEd/\hbar$ is the Bloch frequency and τ_{eff} an effective scattering time). Furthermore, we focus on the tunneling resonance by including only resonant contributions in the calculation of the off-diagonal elements $f_\nu^{\nu'}$ (with $\nu \neq \nu'$). These steps of our approach have been described in more detail in reference [14]. The WS ladder representation of the density matrix is obtained by a Fourier transformation

$$f_\nu^{\nu'}(\boldsymbol{k}) = \sum_{l=-\infty}^{\infty} \mathrm{e}^{\mathrm{i}lk_z d} f_\nu^{\nu'}(\boldsymbol{k}_\perp, l). \tag{6}$$

This equation expresses the periodicity of the solution $f_\nu^{\nu'}(\boldsymbol{k})$ along the field direction k_z. The kinetic equation (1) is treated in this representation. To account for tunneling appropriately, the quantity

$$\widetilde{f}_\nu^{\nu'}(\boldsymbol{k}) = \widetilde{q}_{\nu\nu'}(\boldsymbol{k}) f_\nu^{\nu'}(\boldsymbol{k}), \tag{7}$$

together with the abbreviations

$$\widetilde{q}_{\nu\nu'}(\boldsymbol{k}) = \exp\left\{ -\frac{\mathrm{i}}{eE}\int_0^{k_z} \mathrm{d}k_z' [\varepsilon_\nu(\boldsymbol{k}_\perp, k_z') - \varepsilon_{\nu'}(\boldsymbol{k}_\perp, k_z') - \varepsilon_{\nu\nu'}(\boldsymbol{k}_\perp)] \right\}, \tag{8}$$

$$\varepsilon_{\nu\nu'}(\boldsymbol{k}_\perp) = \frac{d}{2\pi}\int_0^{2\pi/d} \mathrm{d}k_z \left[\varepsilon_\nu(\boldsymbol{k}) - \varepsilon_{\nu'}(\boldsymbol{k})\right] \tag{9}$$

are introduced. The resulting set of equations for the elements of the density matrix have already been derived and solved in reference [14] within the relaxation-time approximation. As scattering plays an essential role, both for the field-induced carrier redistribution and the carrier transport, it is necessary to treat scattering in a more realistic approach. This is the main objective of the present paper.

In our approach, tunneling is described by the off-diagonal elements $f_\nu^{\nu'}$ of the density matrix, which are introduced into the set of kinetic equations *via* the dipole matrix and specific scattering contributions. The dipole matrix elements constitute coherent tunneling through the SL barriers including resonant tunneling without introducing any characteristic tunneling time. Alternatively, these effects could be described by the exact eigenstates of the diagonalized interaction free Hamiltonian. On the contrary, the scattering-induced off-diagonal elements give rise to completely other effects like dissipation and lifetime broadening of the tunneling resonance. A semiclassical description of this broadening is justified as quantum contributions to these transitions, as, *e.g.*, electro-phonon resonances, do not play any role in the stationary regime [5]. To facilitate our analytic approach, we describe the broadening of the tunneling resonance by a phenomenological scattering time parameter τ. Let us treat the tunneling resonance between the first and third subband when the component $\widetilde{f}_3^1$ is dominant. A closed equation for this off-diagonal element of the density matrix can be derived. In this equation, the scattering-mediated broadening of the tunneling resonance is described by the scattering probability W_{33}^{11}. Applying the relaxation-time approximation to this specific scattering mechanism, we obtain the analytical result

$$\widetilde{f}_3^1(\boldsymbol{k}_\perp, l) \approx \frac{eE}{\hbar} \frac{q_{13}(l)}{l\Omega - \omega_{31} - \mathrm{i}/\tau} \times \left[f_3^3(\boldsymbol{k}_\perp, 0) - f_1^1(\boldsymbol{k}_\perp, 0) \right], \qquad (10)$$

which is valid at high electric fields ($\Omega\tau_{eff} > 1$), where the intrawell components $f_\nu^{\nu'}(\boldsymbol{k}_\perp, l = 0)$ are most important. The solution (10) is expressed by the transformed dipole matrix element

$$q_{\nu\nu'}(l) = \sum_{k_z} \mathrm{e}^{-\mathrm{i}lk_z d} Q_{\nu\nu'}(k_z) \widetilde{q}_{\nu\nu'}(k_z). \qquad (11)$$

In the next step of our calculation, the occupation numbers $n_\nu = \sum_{\boldsymbol{k}_\perp} f_\nu^\nu(\boldsymbol{k}_\perp, l = 0)$ have to be determined from the diagonal elements of the density matrix. To calculate the field-mediated carrier redistribution, we focus on scattering on polar-optical phonons described by the Fröhlich-type Hamiltonian, in which the coupling matrix elements $\gamma_{\nu'\nu}$ have to be specified. In spite of screening (or dynamical screening) this is not a trivial task for the multiple subband SL, even when the bulk-phonon model is accepted for an approximate description. We think that a realistic treatment of the smooth wavenumber dependence of the screened coupling constants is not necessary to describe the main features of the QCL structure. This impression is confirmed by experimental studies of intersubband magnetophonon resonances in QCL structures [17,18], which demonstrate that the laser operation depends sensitively on a possible detuning of the electron – longitudinal optical phonon scattering channel and not on the details of the scattering matrix elements. Therefore, in our more qualitative analysis, the wavenumber dependence of the coupling constants is neglected. In addition, in the applied one-electron picture valid in the limit of low carrier concentrations, the Coulomb interaction is not taken into account. Using the expressions for the scattering probabilities from Appendix A and neglecting intracollisional field effects, we obtain after a tedious but straightforward calculation the set of linear equations

$$A(n_1 - n_3) = -a_1 n_1 + a_2 n_2 + a_3 n_3, \qquad (12)$$

$$b_1 n_1 - b_2 n_2 + b_3 n_3 = 0, \qquad (13)$$

$$n_1 + n_2 + n_3 = 1, \qquad (14)$$

in which resonant tunneling is described by the quantity

$$A = \frac{2\hbar}{m^* a^2 \omega_0^2 \tau} \left(\frac{Q_{13}}{d} \right)^2 (1 - \mathrm{e}^{-\beta}) \times \sum_{l=-\infty}^{\infty} \frac{\Phi_l^2 \left([\Delta_3 - \Delta_1]/[2\hbar\Omega] \right)}{(l\Omega\tau - \varepsilon_{31}\tau/\hbar)^2 + 1} \cdot \qquad (15)$$

Here, we introduced the frequency of polar-optical phonons ω_0, the temperature parameter $\beta = \hbar\omega_0/k_B T$, and the lateral lattice constant a. The character of the function $\Phi(x)$ depends on whether the SL unit cell is symmetric or not. We obtain

$$\Phi_l(x) = \begin{cases} J_l(x), & \text{if} \quad Q_{13}(l=0) \neq 0 \\ J_{l-1}(x) - J_{l+1}(x), & \text{if} \quad \begin{cases} Q_{13}(l=0) = 0 \\ Q_{13}(l=\pm 1) \neq 0 \end{cases} \end{cases}, \qquad (16)$$

where $J_l(x)$ denotes the Bessel function. The field-dependent coefficients in the final equations (12) and (13) are given in Appendix B.

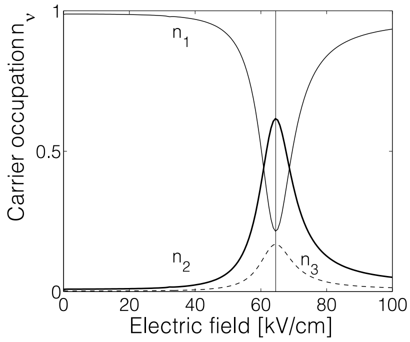

Fig. 1. Carrier occupation n_1 (solid line), n_2 (thick solid line), and n_3 (dashed line) as a function of the electric field for $T = 77$ K. The position of the tunneling resonance is marked by a vertical line. The following model parameters have been used in the calculation: $\Delta_1 = 1$ meV, $\Delta_2 = 2$ meV, $\Delta_3 = 4$ meV, $\varepsilon_{g_1} = 25$ meV, $\varepsilon_{g_2} = 35$ meV, $\tau = 0.5$ ps, and $d = 10$ nm. The SL unit cell is assumed to be symmetric ($Q_{13}(l = 0) = 0$). We used $Q_{13}(l = 1) = 0.2$ nm.

3 Results

The set of linear equations (12) to (14), with coefficients defined in Appendix B, is numerically solved for a SL with a symmetric unit cell [$Q_{13}(l = 0) = 0$ but $Q_{13}(l = 1) \neq 0$]. In the calculations, GaAs bulk parameters are used for the effective mass m^*, the lattice constant a, and the frequency ω_0 of polar-optical phonons. Due to the more qualitative character of our approach, we cannot predict an effective device design based on a given heterostructure. This would require the numerical consideration of more realistic models with no free parameters as initiated by Iotti and Rossi [5].

Figure 1 shows the subband occupation n_ν as a function of the electric field for $T = 77$ K. We focus on the tunneling resonance at $eEd = \varepsilon_{31}$ marked by a vertical line in Figure 1. At this resonance, there is a remarkable carrier redistribution between the subbands. A population inversion is observed between the lowest and the second subband. This inversion is due to resonant tunneling described by the term on the left hand side of equation (12). If this tunneling contribution is absent ($Q_{13} \to 0$), an intrinsic population inversion cannot occur. The emergence of an intrinsic population inversion is also hampered by scattering-mediated broadening. With increasing lifetime

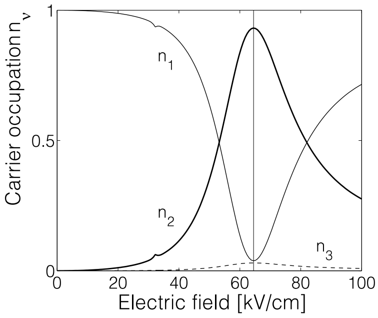

Fig. 2. Carrier occupation n_ν of the SL subbands as a function of the electric field for $T = 30$ K. All other parameters are the same as in Figure 1.

broadening described by the parameter τ, the tunneling resonance becomes smeared out, which eventually prevents the occurrence of an inversion. This happens only in the case when the *ad-hoc* broadening parameter τ of the tunneling resonance becomes much smaller than all other inter- and intrasubband scattering times. Nevertheless, the width of the tunneling resonance is an important parameter of the QCL design, which should be treated in more detail in future work. In the considered temperature regime, the tunneling contribution given by the factor A on the left hand side of equation (12) is practically independent of temperature. The temperature dependence of the population inversion results from scattering-mediated intra- and intersubband transitions described by the coefficients a_i and b_i in equations (12) and (13), respectively. Explicit expressions for these quantities are presented in Appendix B. Figure 2 shows the field dependence of the carrier occupation for $T = 30$ K (all other parameters are the same as in Fig. 1). As expected, the tunneling resonance becomes much more pronounced, when the temperature decreases. In addition, the electric field region, where an intrinsic population inversion occurs, enlarges considerably with decreasing temperature and covers an appreciable interval ranging from about 50 to 80 kV/cm. The qualitative behaviour of the field-induced carrier redistribution at the tunneling resonance agrees with our former results derived within the constant relaxation-time approximation [13,14]. However, to obtain more detailed information about the tunneling resonance and its temperature dependence, a realistic treatment of inelastic scattering is necessary. This allows the determination of the temperature-dependent electric field region, where the inversion occurs. In addition, one can answer the question, whether an inversion may appear at room temperature, too.

4 Summary

The field-induced carrier redistribution in multiband SLs has been studied on the basis of the density matrix approach. A SL with three occupied subbands has been treated within a tight-binding model. The applied electric field is strong enough to establish a tunneling resonance between the first and third subband. Contrary to previous approaches [13,14], which relied on the relaxation-time approximation, scattering on polar-optical phonons has been described within a more realistic model. At the tunneling resonance $eEd = \varepsilon_{31}$, an intrinsic population inversion is observed, which may be used for the implementation of injectorless QCLs. The character of the population inversion depends both on the details of resonant tunneling and the scattering-induced carrier transitions. Our scattering model allows a detailed study of the temperature dependent width and height of the tunneling resonance, which gives rise to a population inversion. Moreover, it is possible to derive conditions for the appearance of an inversion at room temperature.

In our approach, there are still some phenomenological parameters such as the constant dipole matrix element Q_{13} and the scattering time τ for tunneling transitions. More progress is expected from a rigorous microscopic approach with no adjustable parameters.

The authors acknowledge partial financial support by the Deutsches Zentrum für Luft- und Raumfahrt.

Appendix A

In principle, our approach allows a detailed analysis of the field-induced carrier redistribution. The main ingredient of such a full microscopic treatment represents the scattering probability. For further studies, the relevant contributions are given here in its most general form. The intrasubband scattering probabilities of the SL are expressed by

$$
\begin{aligned}
W^{\nu\nu}_{\nu\nu}(\boldsymbol{k}',\boldsymbol{k}) &= 2\mathrm{Re}\sum_{\boldsymbol{q}} \omega_{\boldsymbol{q}}^2 \mid \gamma_{\nu\nu}(\boldsymbol{k},\boldsymbol{q}) \mid^2 \int_0^\infty \mathrm{d}t \mathrm{e}^{-st} \\
&\times \exp\left(\frac{\mathrm{i}}{\hbar}\int_0^t \mathrm{d}\tau \left[\varepsilon_\nu\left(\boldsymbol{k}+\boldsymbol{q}-\frac{eE}{\hbar}\tau\right) - \varepsilon_\nu\left(\boldsymbol{k}-\frac{eE}{\hbar}\tau\right)\right]\right) \\
&\times \left\{\delta_{\boldsymbol{k}',\boldsymbol{k}+\boldsymbol{q}-e\boldsymbol{E}t/\hbar}[(N_{\boldsymbol{q}}+1)\mathrm{e}^{-\mathrm{i}\omega_{\boldsymbol{q}}t} + N_{\boldsymbol{q}}\mathrm{e}^{\mathrm{i}\omega_{\boldsymbol{q}}t}]\right. \\
&\left. - \delta_{\boldsymbol{k}',\boldsymbol{k}-e\boldsymbol{E}t/\hbar}[(N_{\boldsymbol{q}}+1)\mathrm{e}^{\mathrm{i}\omega_{\boldsymbol{q}}t} + N_{\boldsymbol{q}}\mathrm{e}^{-\mathrm{i}\omega_{\boldsymbol{q}}t}]\right\} \\
&- 2\mathrm{Re}\sum_{\boldsymbol{q}} \omega_{\boldsymbol{q}}^2 \int_0^\infty \mathrm{d}t \mathrm{e}^{-st} \delta_{\boldsymbol{k}',\boldsymbol{k}-e\boldsymbol{E}t/\hbar} \\
&\times [(N_{\boldsymbol{q}}+1)\mathrm{e}^{\mathrm{i}\omega_{\boldsymbol{q}}t} + N_{\boldsymbol{q}}\mathrm{e}^{-\mathrm{i}\omega_{\boldsymbol{q}}t}] \left\{ \mid \gamma_{\nu_1\nu}(\boldsymbol{k},\boldsymbol{q}) \mid^2 \right. \\
&\times \exp\left(\frac{\mathrm{i}}{\hbar}\int_0^t \mathrm{d}\tau \left[\varepsilon_{\nu_1}\left(\boldsymbol{k}+\boldsymbol{q}-\frac{eE}{\hbar}\tau\right) - \varepsilon_\nu\left(\boldsymbol{k}-\frac{eE}{\hbar}\tau\right)\right]\right) \\
&+ \mid \gamma_{\nu_2\nu}(\boldsymbol{k},\boldsymbol{q}) \mid^2 \\
&\left. \times \exp\left(\frac{\mathrm{i}}{\hbar}\int_0^t \mathrm{d}\tau \left[\varepsilon_{\nu_2}\left(\boldsymbol{k}+\boldsymbol{q}\frac{eE}{\hbar}\tau\right) - \varepsilon_\nu\left(\boldsymbol{k}-\frac{eE}{\hbar}\tau\right)\right]\right)\right\},
\end{aligned}
\tag{17}
$$

where $\gamma_{\nu\nu'}$ denote intra- and intersubband coupling constants of the electron-phonon interaction. The parameter s goes to zero after the integral over the time variable t has been carried out. The scattering probabilities depend on the electric field (intra-collisional field effects). In equation (17), $N_{\boldsymbol{q}}$ denotes the Bose distribution function of bulk phonons. The relevant intersubband components of the scattering probability are given by

$$W_{\nu'\nu}^{\nu'\nu}(\boldsymbol{k}',\boldsymbol{k}) = 2\mathrm{Re}\sum_{\boldsymbol{q}}\omega_{\boldsymbol{q}}^2 \mid \gamma_{\nu'\nu}(\boldsymbol{k},\boldsymbol{q}) \mid^2 \int_0^\infty \mathrm{d}t\mathrm{e}^{-st}$$
$$\times \exp\left(\frac{\mathrm{i}}{\hbar}\int_0^t \mathrm{d}\tau\left[\varepsilon_{\nu'}(\boldsymbol{k}+\boldsymbol{q}-\frac{eE}{\hbar}\tau)-\varepsilon_\nu(\boldsymbol{k}-\frac{eE}{\hbar}\tau)\right]\right)$$
$$\times\,\delta_{\boldsymbol{k}',\boldsymbol{k}+\boldsymbol{q}-e\boldsymbol{E}t/\hbar}[(N_{\boldsymbol{q}}+1)\mathrm{e}^{-\mathrm{i}\omega_{\boldsymbol{q}}t}+N_{\boldsymbol{q}}\mathrm{e}^{\mathrm{i}\omega_{\boldsymbol{q}}t}]. \quad (18)$$

The treatment of the field-induced carrier redistribution in Section 2 is based on a quasi-classical picture, in which intra-collisional field effects are not taken into account.

Appendix B

The final equations (12) and (13) are derived by a Fourier transformation of the kinetic equations according to equation (6) and by carrying out the remaining $\boldsymbol{k}_\perp$ integrals. When the momentum dependence of the coupling terms $\gamma_{\nu\nu'}$ is neglected, the $\boldsymbol{k}_\perp$ integrals can be replaced by integrals over an energy variable $\varepsilon = \hbar^2\boldsymbol{k}_\perp^2/2m^*$. We obtain for the coefficients in equations (12) and (13)

$$a_1 =\mid \gamma_{11}\mid^2\sum_l g_{11}(l)\left[1-\mathrm{e}^{-\frac{l\hbar\Omega}{k_BT}}\right]\Big\{\mathrm{e}^{-\beta}$$
$$\times\left[1-\Theta(-l\hbar\Omega-\hbar\omega_0)\left(1-\mathrm{e}^{\frac{l\hbar\Omega+\hbar\omega_0}{k_BT}}\right)\right]$$
$$+\left[1-\Theta(-l\hbar\Omega+\hbar\omega_0)\left(1-\mathrm{e}^{\frac{l\hbar\Omega-\hbar\omega_0}{k_BT}}\right)\right]\Big\}$$
$$+\mid \gamma_{21}\mid^2\sum_l g_{21}(l)\Big\{\mathrm{e}^{-\beta}$$
$$\times\left[1-\Theta(\varepsilon_{21}-l\hbar\Omega-\hbar\omega_0)\left(1-\mathrm{e}^{\frac{l\hbar\Omega+\hbar\omega_0-\varepsilon_{21}}{k_BT}}\right)\right]$$
$$+\left[1-\Theta(\varepsilon_{21}-l\hbar\Omega+\hbar\omega_0)\left(1-\mathrm{e}^{\frac{l\hbar\Omega-\hbar\omega_0-\varepsilon_{21}}{k_BT}}\right)\right]\Big\}$$
$$+\mid \gamma_{31}\mid^2\sum_l g_{31}(l)\Big\{\mathrm{e}^{-\beta}$$
$$\times\left[1-\Theta(\varepsilon_{31}-l\hbar\Omega-\hbar\omega_0)\left(1-\mathrm{e}^{\frac{l\hbar\Omega+\hbar\omega_0-\varepsilon_{31}}{k_BT}}\right)\right]$$
$$+\left[1-\Theta(\varepsilon_{31}-l\hbar\Omega+\hbar\omega_0)\left(1-\mathrm{e}^{\frac{l\hbar\Omega-\hbar\omega_0-\varepsilon_{31}}{k_BT}}\right)\right]\Big\}, \quad (19)$$

$$a_\nu =\mid \gamma_{\nu1}\mid^2\sum_l g_{\nu1}(l)\left[1-\mathrm{e}^{-\frac{\varepsilon_{\nu1}-l\hbar\Omega}{k_BT}}\right]\Big\{\mathrm{e}^{-\beta}$$
$$\times\left[1-\Theta(\varepsilon_{\nu1}-l\hbar\Omega-\hbar\omega_0)\left(1-\mathrm{e}^{\frac{l\hbar\Omega+\hbar\omega_0-\varepsilon_{\nu1}}{k_BT}}\right)\right]$$
$$+\left[1-\Theta(\varepsilon_{\nu1}-l\hbar\Omega+\hbar\omega_0)\left(1-\mathrm{e}^{\frac{l\hbar\Omega-\hbar\omega_0-\varepsilon_{\nu1}}{k_BT}}\right)\right]\Big\}, \quad (20)$$

$$b_2 =\mid \gamma_{22}\mid^2\sum_l g_{22}(l)\left[1-\mathrm{e}^{-\frac{l\hbar\Omega}{k_BT}}\right]\Big\{\mathrm{e}^{-\beta}$$
$$\times\left[1-\Theta(-l\hbar\Omega-\hbar\omega_0)\left(1-\mathrm{e}^{\frac{l\hbar\Omega+\hbar\omega_0}{k_BT}}\right)\right]$$
$$+\left[1-\Theta(-l\hbar\Omega+\hbar\omega_0)\left(1-\mathrm{e}^{\frac{l\hbar\Omega-\hbar\omega_0}{k_BT}}\right)\right]\Big\}$$
$$+\mid \gamma_{21}\mid^2\sum_l g_{21}(l)\Big\{\mathrm{e}^{-\beta}$$
$$\times\left[1-\Theta(-\varepsilon_{21}-l\hbar\Omega-\hbar\omega_0)\left(1-\mathrm{e}^{\frac{l\hbar\Omega+\hbar\omega_0+\varepsilon_{21}}{k_BT}}\right)\right]$$
$$+\left[1-\Theta(-\varepsilon_{21}-l\hbar\Omega+\hbar\omega_0)\left(1-\mathrm{e}^{\frac{l\hbar\Omega-\hbar\omega_0+\varepsilon_{21}}{k_BT}}\right)\right]\Big\}$$
$$+\mid \gamma_{32}\mid^2\sum_l g_{32}(l)\Big\{\mathrm{e}^{-\beta}$$
$$\times\left[1-\Theta(\varepsilon_{32}-l\hbar\Omega-\hbar\omega_0)\left(1-\mathrm{e}^{\frac{l\hbar\Omega+\hbar\omega_0-\varepsilon_{32}}{k_BT}}\right)\right]$$
$$+\left[1-\Theta(\varepsilon_{32}-l\hbar\Omega+\hbar\omega_0)\left(1-\mathrm{e}^{\frac{l\hbar\Omega-\hbar\omega_0-\varepsilon_{32}}{k_BT}}\right)\right]\Big\}, \quad (21)$$

$$b_1 =\mid \gamma_{21}\mid^2\sum_l g_{21}(l)\mathrm{e}^{-\frac{\varepsilon_{21}+l\hbar\Omega}{k_BT}}\Big\{\mathrm{e}^{-\beta}$$
$$\times\left[1-\Theta(-\varepsilon_{21}-l\hbar\Omega-\hbar\omega_0)\left(1-\mathrm{e}^{\frac{l\hbar\Omega+\hbar\omega_0+\varepsilon_{21}}{k_BT}}\right)\right]$$
$$+\left[1-\Theta(-\varepsilon_{21}-l\hbar\Omega+\hbar\omega_0)\left(1-\mathrm{e}^{\frac{l\hbar\Omega-\hbar\omega_0+\varepsilon_{21}}{k_BT}}\right)\right]\Big\}, \quad (22)$$

$$b_3 =\mid \gamma_{32}\mid^2\sum_l g_{32}(l)e^{\frac{\varepsilon_{32}-l\hbar\Omega}{k_BT}}\Big\{\mathrm{e}^{-\beta}$$
$$\times\left[1-\Theta(\varepsilon_{32}-l\hbar\Omega-\hbar\omega_0)\left(1-\mathrm{e}^{\frac{l\hbar\Omega+\hbar\omega_0-\varepsilon_{32}}{k_BT}}\right)\right]$$
$$+\left[1-\Theta(\varepsilon_{32}-l\hbar\Omega+\hbar\omega_0)\left(1-\mathrm{e}^{\frac{l\hbar\Omega-\hbar\omega_0-\varepsilon_{32}}{k_BT}}\right)\right]\Big\}, \quad (23)$$

where the functions

$$g_{\nu\nu'}(l) = \frac{1}{\pi}\int_0^\infty \mathrm{d}z\cos(lz)J_0\left(\frac{\Delta_\nu}{\hbar\Omega}\sin\frac{z}{2}\right)$$
$$\times J_0\left(\frac{\Delta_{\nu'}}{\hbar\Omega}\sin\frac{z}{2}\right) \quad (24)$$

and the step function Θ have been introduced.

References

1. J. Faist, F. Capasso, D. Sivco, A. Hutchinson, A. Cho, Science **264**, 553 (1994)
2. R.F. Kazarinov, R.A. Suris, Fiz. Tekh. Poluprovodn. **5**, 797 (1971) [Sov. Phys. Semicond. **5**, 707 (1971)]
3. N. Ulbrich, G. Scarpa, G. Böhm, G. Abstreiter, M.C. Aman, Appl. Phys. Lett. **80**, 4312 (2002)
4. S. Tortora, F. Compagnone, A.D. Carlo, P. Lugli, Physica E **7**, 20 (2000)
5. R. Iotti, F. Rossi, Phys. Rev. Lett. **87**, 146603 (2001)
6. F. Compagnone, A.D. Carlo, P. Lugli, Appl. Phys. Lett. **80**, 920 (2002)
7. P. Kinsler, R.W. Kelsall, P. Harrison, J. Appl. Phys. **91**, 904 (2002)
8. V.B. Gorfinkel, S. Luryi, B. Gelmont, IEEE J. Quantum Electron. **32**, 1995 (1996)
9. B. Gelmont, V.B. Gorfinkel, S. Luryi, Appl. Phys. Lett. **68**, 2171 (1996)
10. M. Kucharczyk, M.S. Wartak, P. Weetman, P. Lau, J. Appl. Phys. **86**, 3218 (1999)
11. S. Blaser, L. Diehl, M. Beck, J. Faist, U. Oesterle, J. Xu, S. Barbieri, F. Beltram, IEEE J. Quantum Electron. **37**, 448 (2001)
12. K. Donovan, P. Harrison, R.W. Kelsall, J. Appl. Phys. **89**, 3084 (2001)
13. P. Kleinert, V.V. Bryksin, Phys. Rev. B **63**, 193303 (2001)
14. P. Kleinert, V.V. Bryksin, Physica E **11**, 332 (2001)
15. J. Hader, T. Meier, S.W. Koch, F. Rossi, N. Linder, Phys. Rev. B **55**, 13799 (1997)
16. P. Kleinert, J. Phys. Cond. Matt. **12**, 8467 (2000)
17. D. Smirnov, C. Becker, O. Drachenko, V.V. Rylkov, H. Page, J. Leotin, C. Sirtori, Phys. Rev. B **66**, 121305 (2002)
18. C. Becker, C. Sirtori, O. Drachenko, V. Rylkov, D. Smirnov, J. Leotin, Appl. Phys. Lett. **81**, 2941 (2002)